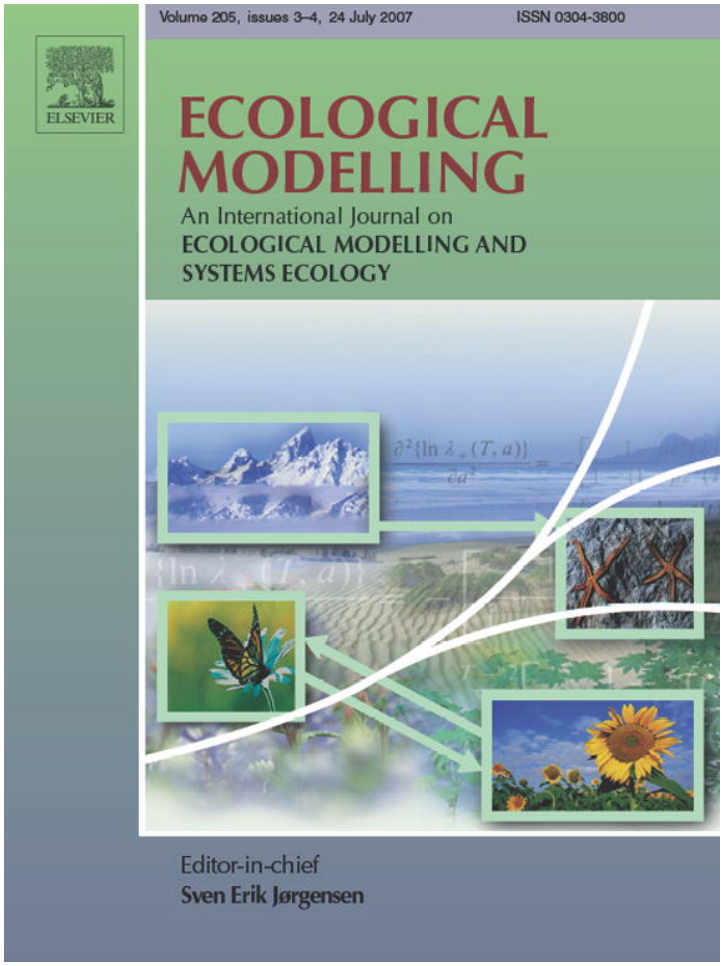

ECOLOGICAL MODELLING 205 (2007) 475–491

available at www.sciencedirect.com

ScienceDirect

journal homepage: www.elsevier.com/locate/ecolmodel

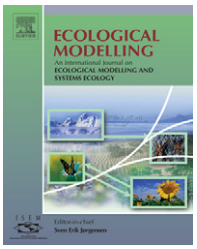

A process-based model for methane emission from flooded rice paddy systems

Shangping Xu[a,*], *Peter R. Jaffé*[b], *Denise L. Mauzerall*[c]

[a] *Department of Geosciences, University of Wisconsin, Milwaukee, WI 53211, United States*
[b] *Department of Civil and Environmental Engineering, Princeton University, Princeton, NJ 08544, United States*
[c] *Science, Technology and Environmental Policy Program, Woodrow Wilson School of Public and International Affairs, Princeton University, Princeton, NJ 08544, United States*

ARTICLE INFO

Article history:
Received 25 October 2005
Received in revised form
23 February 2007
Accepted 13 March 2007
Published on line 19 April 2007

Keywords:
Methane
Rice paddy
Global warming
Model

ABSTRACT

Methane is the second most important greenhouse gas after carbon dioxide. Rice paddy soils release approximately 15–20% of total methane emitted to the atmosphere. A process-based methane emission model was developed for rice paddy systems that highlights plant mediated methane transport. Sequential utilization of alternative electron acceptors such as oxygen, nitrate, Mn(IV), Fe(III) and sulfate in flooded soils is included and permits examination of the effects of fertilizer application and field drainage on methane emissions. Acetate and hydrogen, two representative electron donors produced from the biologically mediated decomposition of solid organic matter, are assumed to be the substrates driving the electron transfer processes. Effects of temperature on reaction kinetics and diffusion processes are based on empirical relationships observed in the laboratory and field. Other processes considered include the exudation of organic carbon and radial release of oxygen from roots, the infiltration flow induced by plant transpiration, the growth dynamics of rice plants, the vertical distribution of soil organic carbon and root biomass, dieback of roots, and loss of gaseous species through ebullition. The performance of the model is evaluated using methane flux data collected in Chongqing and Sichuan, China. Model simulations reveal that although hybrid rice cultivars are several times more efficient in mediating methane transport than traditional tall cultivars at seedling stage, the development of methane transport capacity over the growing season leads to a relatively small difference in total seasonal methane flux (~15%) among fields planted with tall and hybrid cultivars. Application of nitrate fertilizer at a rate of 64 kg N/ha (about 50% of total nitrogen applied at the Chongqing site) could reduce methane emission by 7%. By converting both iron and manganese to oxidized forms, pre-season drainage is found to be able to reduce methane emissions by 8–10%. A 1-week drainage of a rice field during the growing season could further reduce the methane emission by 22–23% and might be a very promising methane-emission mitigation technique, since such drainage practices can also conserve water and improve rice yields. This model will be implemented on a national scale to establish national methane emission inventories and to evaluate the feasibility and cost-effectiveness of various mitigation options that could vary from site to site.

* *Corresponding author*. Tel.: +1 414 229 6148; fax: +1 414 228 5452.
E-mail address: xus@uwm.edu (S. Xu).
0304-3800/$ – see front matter © 2007 Elsevier B.V. All rights reserved.
doi:10.1016/j.ecolmodel.2007.03.014

1. Introduction

Methane is currently the second most important greenhouse gas accounting for 15–20% of anthropogenic radiative forcing (Rodhe, 1990; IPCC, 1995a,b). Anthropogenic sources are responsible for about 70% of total methane emission (IPCC, 1995a,b). With an estimated annual emission of 25–100 Tg of methane, rice paddies represent one of the major contributors to atmospheric methane (IPCC, 1995a,b).

Rice is the world's most important food source and its cultivation area has increased from 104 million ha to 148 million ha over the last half century (Aulakh et al., 2001a,b,c). About 131 million ha rice paddies are flooded by irrigation or rainwater during the growing season. Once flooded, anaerobic conditions quickly develop in rice paddy soils resulting in the sequential utilization of a series of electron acceptors, such as oxygen, nitrate, Mn(IV), Fe(III) and sulfate. Methane production starts under highly reducing conditions after alternative electron acceptors have been depleted.

Methane produced in rice paddy soils is emitted to the atmosphere by three pathways: molecular diffusion, ebullition as gas bubbles, and rice-mediated transport (Hosono and Nouchi, 1997). Contributions from individual pathways vary over time and space, and many researchers have documented that rice-mediated transport is the major pathway potentially accounting for more than 90% of the total methane emitted from soils over the growing season (Cicerone and Shetter, 1981; Butterbach-Bahl et al., 1997; Hosono and Nouchi, 1997). A fraction of methane produced in soils may be subject to oxidation in the rhizosphere, either aerobically by oxygen released from plant roots or anaerobically by other electron acceptors such as indigenous ferric iron or sulfate (usually from fertilizer) (Iversen and Jorgensen, 1985).

Emission of methane from rice paddies is affected by a variety of agronomic and environmental factors including physiological characteristics of rice cultivars, applications of both inorganic and organic fertilizers (e.g., manure), water management practices, soil physicochemical and geochemical properties, air and soil temperature, and composition and activity of soil microorganisms (Bodelier et al., 2000). Substantial temporal and spatial variations in methane fluxes have been observed by many investigators (Schutz et al., 1990; Minami, 1995; Yang and Chang, 1999; Wassmann et al., 2000; Kruger et al., 2001). Such variations make methane-flux estimations from rice paddies more difficult, and complicate the assessment of its effects on global climate change.

Methane emission models have been used to estimate methane fluxes under a range of environmental and agronomic conditions, to identify key parameters and processes that control methane fluxes from rice paddies, and to explore mitigation strategies that lead to reductions in methane emissions. (e.g., Bachelet et al., 1995; Cao et al., 1998; Huang et al., 1998a,b; Knox et al., 2000; Matthews et al., 2000a,b; Van Bodegom et al., 2002; Yan et al., 2003).

Based on the insights gained into the mechanisms underlying the production, oxidation, and emission of methane in wetland systems, many process-based methane flux models have been developed during the last decade (e.g., Cao et al., 1995; Kern et al., 1997; Huang et al., 1998a,b; Arah and Kirk, 2000; Matthews et al., 2000a,b; Walter and Heimann, 2000; Segers and Leffelaar, 2001a,b; Segers et al., 2001; Van Bodegom et al., 2001a,b; Li et al., 2002a,b; Kettunen, 2003; Yan et al., 2003). Although the transport of methane by plants was included in many of these models, it was often described by a transport coefficient (e.g., Walter and Heimann, 2000; Van Bodegom et al., 2001a,b), and the incorporation of the details of plant-mediated transport in methane emission models is still uncommon. Highlights of this one-dimensional process-based methane emission model include: (i) methane transport mediated through rice plants, as well as its temperature dependency, is accounted for based on recently reported experimental results (Hosono and Nouchi, 1997; Aulakh et al., 2000a,b; Aulakh et al., 2002). This allows for the examination of the impacts of rice cultivar selection on methane emission; (ii) the vertical distribution of organic carbon, the major driving force for methane production in rice paddy soils, was compiled based on 626 measurements in China and incorporated into the model; (iii) infiltration flow induced by plant transpiration, which leads to the penetration of oxygen in the overlying water and redistribution of dissolved species in the rhizosphere and can have significant impact on the biogeochemical processes in flooded soils (Xu et al., 2004; Xu and Jaffe, 2006), is considered in this model formulation; (iv) the model includes the sequential utilization of all the major electron acceptors (e.g., oxygen, nitrate, Mn(IV), Fe(III) and sulfate) relevant to methane production, oxidation, and emission in rice paddy systems, permitting the evaluation of the impact of various agricultural practices, such as field drainage and fertilizer application, on methane emission.

The performance of the model was evaluated using field observations obtained over several years and for different soils, rice cultivars, and agricultural practices. Attempts were then made to identify the impacts of some key processes and parameters, such as rice cultivar selection and field drainage, on methane fluxes from rice paddies and to assess the effectiveness of some methane emission mitigation options. The goal is to implement this model for rice paddy fields in China, the largest rice producer, through the integration of remote sensing data and up-scaling GIS techniques (Yu et al., 2001; Yue et al., 2003) to establish methane emission inventories and to evaluate the feasibility and cost-effectiveness of site-specific mitigation options in the framework of sustainable agriculture (Bachelet et al., 1995; Ulgiati et al., 2006).

2. Model structure

The one-dimensional non-steady-state model formulation is designed to incorporate the coupled transport and reaction of both dissolved and solid species in the vertical dimension, while horizontal homogeneity is assumed. The transport and reaction of each chemical species is constrained by its mass balance and individual chemical species are linked though the appropriate reaction terms.

2.1. *Mass balance equations*

The mass balance of each species (solid and dissolved) is described by a one-dimensional, transport-reaction equation.

The transport of a dissolved species i, assuming a constant porosity, can be described by the following equation:

$$\frac{\partial}{\partial t}C_i^{aq} = -\frac{\partial}{\partial z}[V(z)C_i^{aq}] + \frac{\partial}{\partial z}\left[D(z)\frac{\partial C_i^{aq}}{\partial z}\right] + \frac{\sum R}{\phi} \quad (1)$$

where t is the time, ϕ represents porosity, C_i^{aq} means concentration of species i in the liquid phase, V the vertical infiltration velocity of water, which is a function of depth and is influenced by plant transpiration, z the soil depth, $D(z)$ represents hydrodynamic dispersion coefficient for species i, and ΣR is the sum of reactions.

Diffusion of methane from the soil solution into the roots is the first step in its transport through the rice aerenchyma system (Nouchi et al., 1990). The mass balance equation for methane (Eq. (2)) explicitly includes such a transport term, Φ:

$$\frac{\partial}{\partial t}C^{aq} = -\frac{\partial}{\partial z}[V(z)C^{aq}] + \frac{\partial}{\partial z}\left[D(z)\frac{\partial C^{aq}}{\partial z}\right] - \frac{\Phi(C^{aq}, D_{rs}, L_{rw}, \frac{C^r}{H}, A(z), \eta)}{\phi} + \frac{\sum R}{\phi} \quad (2)$$

where D_{rs} is the diffusion coefficient of methane across the root epidermis, H the Henry's constant for methane, C^r the methane concentration in the root, L_{rw} the thickness of root epidermis, $A(z)$ the average root surface area per unit volume of soil, and η is an experimentally determined methane transport capacity coefficient. Other parameters are identical to Eq. (1). The details of the plant mediated methane transport term, Φ, will be presented in the sections below.

Transport and reaction of solid species, such as ferric (hydr)oxide, manganese oxide, solid organic carbon and dead roots is described by:

$$\frac{\partial}{\partial t}C_j^s = \frac{\partial}{\partial z}\left(D_b(z)\frac{\partial C_j^s}{\partial z}\right) + \frac{\sum R}{1-\phi} \quad (3)$$

where C_j^s represents the concentration of solid species j, $D_b(z)$ is a physical mixing (bioturbation) coefficient and other parameters are similarly defined.

2.2. Growth dynamics and vertical distribution of rice roots

The growth of rice roots strongly affects methane production, oxidation, and emission since it determines the rates of radial release of oxygen and organic exudates as well as the methane transport capacity. In this research, an empirical rice growth model is applied to simulate rice growth over the growing season based on experimental data obtained under various nutrient supply conditions (Singh et al., 1998; Van Bodegom et al., 2001a,b) (Fig. 1):

$$M_{root} = \begin{cases} \dfrac{M_{max}}{1 + 85.5\, e^{(-13.3 \times time_R)}}, & \text{if } time_R < 0.67 \\ M_{max}\left(1 - \dfrac{time_R - 0.67}{0.33}\right), & \text{if } time_R \geq 0.67 \end{cases} \quad (4)$$

where M_{root} is the dry root mass of one rice plant (g plant^{-1}), M_{max} the maximum dry root biomass per plant (g plant^{-1}),

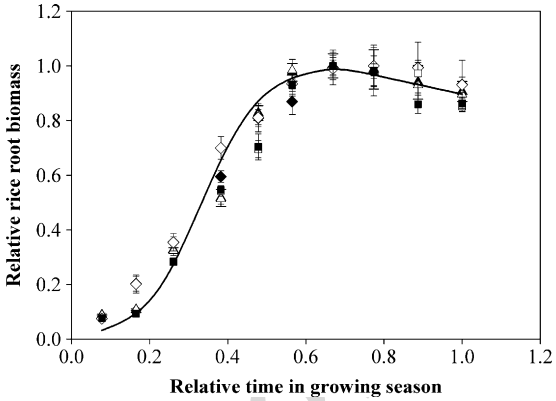

Fig. 1 – Dynamics of rice root growth. Triangle, cultivar Sarju-52; diamond, cultivar Malviya-32; square, cultivar Pant-4. Closed symbols represent data from control fields without fertilizer application and data from fertilized fields are shown in open symbols. Experimental data from Singh et al. (1998). Line represents an empirical model, see text for details.

and $time_R$ is the relative time into the growing season (dimensionless). Since this empirical function does not capture the diurnal variations in the photosynthetic rate of rice plants, this model is not intended to simulate methane fluxes on the diurnal time scale.

The vertical distribution of rice roots has been observed to follow an exponential function (Frenzel et al., 1999; Segers and Leffelaar, 2001a,b):

$$\Gamma = \frac{1}{d}e^{-z/d} \quad (5)$$

where Γ is the root mass distribution, d an empirical value and equals 0.11 m, and z is the soil depth (m). In the model, the total mass of rice roots is assigned to each soil layer according to this function, resulting in a similar relative growth and dieback rate of rice roots at each depth. This function is also applied to determine the vertical distribution of root exudates and methane transport capacity.

2.3. Soil organic matter and its decomposition

Soil organic matter is the driving force for a variety of redox reactions relevant to methane production. In this model, soil organic matter, root dieback, and root exudation are considered as the sources of organic carbon. The formulation of the production of organic substrates in previous methane emission models has been described either via photosynthesis or net primary production functions (Huang et al., 1998a,b; Matthews et al., 2000a,b; Walter and Heimann, 2000; Granberg et al., 2001; Kettunen, 2003), or decomposition kinetics of soil organic matter (Van Bodegom and Scholten, 2001; Van Bodegom et al., 2001a,b). The former formulation has been primarily applied on a regional scale, while the latter was often implemented on smaller spatial scales. In this study, the decomposition kinetics methodology for organic carbon from all sources is adopted due to the spatial scale of concern in this research.

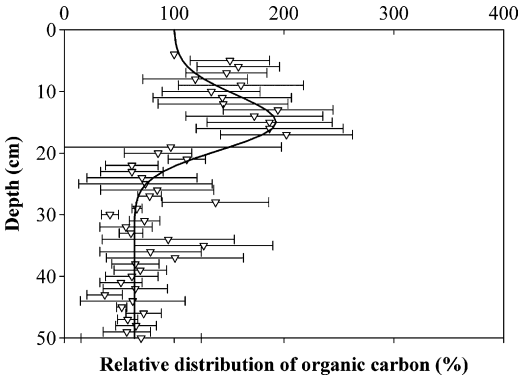

Fig. 2 – Vertical distribution of organic carbon (normalized by the surface carbon content) in China's rice paddy soils. Data are from the National Soil Survey of China, 1993–1996. Solid line represents an empirical model, see text for details.

Usually soil organic matter exhibits significant vertical variations (Jobbagy and Jackson, 2000). To address this, soil organic content of China's rice paddy soils were compiled and the average area-weighted results are shown in Fig. 2 (National Soil Survey of China, 1993–1996). The observed average vertical distribution can be empirically described by the following equation (derived from Fig. 2):

$$C_{\text{carbon}} = \begin{cases} 1 + 0.93 \times e^{-(z-15)^2/40}, & 0 \le z \le 15 \\ 0.64 + 1.29 \times e^{-(z-15)^2/40}, & 15 < z \le 30 \\ 0.64, & 30 < z \le 50 \end{cases} \quad (6)$$

where C_{carbon} is the relative soil carbon content (normalized to surface carbon content, dimensionless), and z is the soil depth in cm. This vertical distribution function is applied by adjusting its amplitude according to measurements conducted at the testing sites.

Under highly reducing conditions, methane is a product of the anaerobic degradation of soil organic matter by bacteria. Conceptually, the degradation pathways of soil organic matter and the production of methane can be summarized by three major steps (Conrad, 1999). Degradation starts with the hydrolysis of organic polymers, and the consequent production of alcohols, fatty acids and hydrogen, both catalyzed by enzymes of fermenting bacteria. Alcohols and fatty acids are then degraded into acetate, hydrogen or formate, and CO_2. The last step is the production of methane from H_2/CO_2 or acetate. Acetate could also be produced from the hydrolysis of organic polymers by homoacetogenic bacteria (Conrad, 1999),

Although the conceptual pathways are largely known, accurate parameterization of the kinetics of methane production has not been well established. Therefore, a simple empirical model describing the degradation of soil organic matter under anaerobic conditions is adopted in this model (Van Bodegom and Scholten, 2001; Van Bodegom et al., 2001a,b). The advantage of this pragmatic treatment is the convenience of mathematical manipulation, while the overall decomposition and utilization kinetics of soil organic matter are captured (Van Bodegom and Scholten, 2001). Briefly, the mineralization of solid organic hydrocarbon (including rice straw, but excluding root dieback and exudation) and the production of acetate and hydrogen can be summarized by Eq. (7) (Van Bodegom and Scholten, 2001):

$$(CH_2O)_n + \tfrac{1}{3}nH_2O \rightarrow \tfrac{1}{3}nCH_3COOH + \tfrac{1}{3}nCO_2 + \tfrac{2}{3}nH_2 \quad (7)$$

In this simplified model, the production of CO_2 reflects the energy used by bacteria that mediate the decomposition process. In reality, low-molecular-weight mineralization products of natural organic matter include a wide variety of organic compounds such as lactic, pyruvic, oxalic, malonic, and succinic acids, propionate and butyrate (Conrad and Klose, 2000; Strobel, 2001). Furthermore, rice root exudates contain various low-molecular-weight organic acids such as malic, tartaric, and succinic acids (Aulakh et al., 2001a,b,c). It is assumed here that substrate utilization kinetics in the production of methane is similar for many small-molecular compounds, and acetate serves as a representative molecule. Methane production rates of soil samples amended with plant exudates appear to be correlated with the total amount of dissolved soil carbon, instead of any individual constituent (Aulakh et al., 2001a,b,c). This suggests that methanogenesis from various readily available organic substrates may be collectively described by a uniform kinetic formulation.

The kinetics of the simplified empirical degradation model for soil organic carbon as described by Eq. (7) has been experimentally determined (Eq. (8)) (Van Bodegom and Scholten, 2001):

$$P_{\text{min}} = C_{\text{min}}(1 - S)K_d\, e^{-K_d \times \text{time}} \quad (8)$$

where P_{min} is the mineralization rate (mol C L^{-1}), S an empirical parameter, and K_d is the relative decomposition rate, defined as:

$$K_d = R\,\text{time}^{-s} \quad (9)$$

where R (unit: time^{s-1}) is also an empirical parameter (Van Bodegom and Scholten, 2001).

Root exudates are important as a readily available carbon source for various microbial activities, including the production of methane (Wang et al., 1997; Lu et al., 1999, 2000; Wang and Adachi, 2000; Aulakh et al., 2001a,b,c; Lu et al., 2002). Here it is assumed that root exudates are in the form of acetate and the exudation rate is a function of root biomass and can be described by an empirical relationship (Eq. (10)) (Wang et al., 1997; Matthews et al., 2000a,b; Aulakh et al., 2001a,b,c):

$$P_{\text{exu}} = 9.2 \times 10^{-4} \times (M_{\text{root}} - 0.8) \quad (10)$$

where P_{exu} is the root exudation rate (mol acetate day^{-1}), and M_{root} is the root dry biomass (g plant^{-1}). This relationship does not capture the diurnal variations in the exudation rate (Fig. 1).

Later in the growing season root dieback occurs and contributes to the soil organic pool. Again, it is assumed here that dead roots are first converted to dissolved organic carbon (acetate) and hydrogen before being utilized by bacteria. For the purpose of simplicity, $(CH_2O)_{106}(NH_3)_{16}(H_3PO_4)$ is used to represent root composition. The kinetics of root decom-

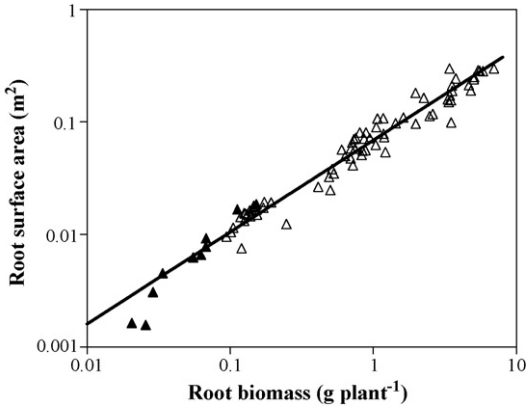

Fig. 3 – Relationship between rice-root surface area and rice-root biomass. Data from Kirk and Du (1997) (closed triangle), Wissuwa and Ae (2001), and Wissuwa (personal communication) (open triangle). Line represents the regression curve, $A = 0.0689M^{0.8162}$, $r^2 = 0.96$.

position is modeled by first-order decay (Van Bodegom et al., 2001a,b) as shown in the following equation:

$$P_{root} = K_{root} M_{root} \quad (11)$$

where P_{root} is the decomposition rate of roots (mol L^{-1} day^{-1}), K_{root} (day^{-1}) the first-order constant and M_{root} is the mass of dead roots (in mol CH_2O L^{-1}). The dieback rate of roots is assumed to be linear (Eq. (4)).

2.4. *Root surface area*

Root surface area is one of the key parameters that determine the flux of methane from soil to rice aerenchyma and thus its overall emission rate. Rice root surface area was also observed to be closely related to the radial oxygen release rate (Colmer, 2003a,b; Kirk, 2003). Data of rice root surface area and root biomass were compiled from the literature (Kirk and Du, 1997; Wissuwa and Ae, 2001) and a power function was found to describe their relationship satisfactorily (Fig. 3 and Eq. (12)):

$$A = 0.0689M^{0.8162} \quad (12)$$

where A is the root surface area (m^2) and M is the root biomass (g). Note that this relationship is based on the surface area and root biomass for one individual plant.

2.5. *Methane transport capacity by rice plants*

Rice plants function like a conductive pipe connecting the rhizosphere and the atmosphere. The model formulation focuses on the diffusion of methane across the soil–root interface, assuming that methane transport inside rice plants is fast enough so that no significant accumulation of methane occurs inside the plants. Therefore, the same form of the power function describing the relationship between root surface area and root biomass should also be used to describe the relationship between methane transport capacity and root biomass. Inspection of experimental data collected for 20 cultivars reveals the following features of methane transport capacity of rice plants (Aulakh et al., 2002): (i) methane transport capacity by rice plants is cultivar dependent and can be grouped into three categories: tall cultivars, dwarf and new plant type (NPT) cultivars, and hybrid cultivars; (ii) there is a drop in methane transport capacity around maturity for tall, dwarf and NPT cultivars. Such a decline has been attributed to blocks in aerenchyma channels due to the dying cells in roots, culm base, and tillers, and bending at the stem–root connection area (Nouchi et al., 1994; Aulakh et al., 2000a,b; Lu et al., 2000; Aulakh et al., 2002). For hybrid cultivars, however, since their sturdier stems can keep the plant in an upright position even at maturity, the decline is less significant or even non-observable (Aulakh et al., 2002); (iii) for dwarf, NPT, and hybrid cultivars, once their root biomass exceeded a certain value, no further increase in methane transport capacity was observed. This is attributed to the resistance from other parts of the plant, such as culm base, and the stem–root connection area; (iv) seedlings of hybrid cultivars are more efficient in mediating methane transport through plants. When root biomass is 1 g, the efficiencies of dwarf/NPT and of tall cultivars are 85% and 28%, respectively, of the efficiency of hybrid cultivars (Fig. 4). However, since there is no further increase in methane transport capacity when root biomass is above a certain value for hybrid cultivars, when root biomass is 5 g, there is virtually no difference in methane transport capacities between tall and hybrid cultivars.

For tall cultivars, either before or around maturity, the power function between root surface area and root biomass can be used satisfactorily to describe methane transport capacity as a function of the root biomass (Fig. 4A). To account for the decline in methane transport capacity around maturity, a methane transport efficiency coefficient, η, is introduced (Eq. (13)).

$$\Phi\left(C^{aq}, D_{rs}, L_{rw}, \frac{C^r}{H}, A(z), \eta\right) = \eta D_{rs} \frac{C^{aq} - (C^r/H)}{L_{rw}} A(z) \quad (13)$$

Around maturity, a linear decline in methane transport capacity and η is assumed and calculated based on experimental data (Fig. 4A and Eq. (14)):

$$\eta = \begin{cases} 1, & \text{before flowering} \\ \left(1 - 0.725\dfrac{t - T_{flowering}}{T_{maturity} - T_{flowering}}\right), & \text{from flowering to maturity} \end{cases} \quad (14)$$

where $T_{maturity}$ and $T_{flowering}$ are, respectively, the maturity time and the flowering time of rice plants.

For dwarf, NPT and hybrid rice cultivars, a maximum effective root biomass (MERB) is defined. When the root biomass exceeds MERB, the methane transport capacity is assumed to be constant. Similarly, the decline in methane transport capacity around plant maturity for dwarf and NPT cultivars is captured by η described by the following equation:

$$\eta = \begin{cases} 1, & \text{before flowering} \\ \left(1 - 0.509\dfrac{t - T_{flowering}}{T_{maturity} - T_{flowering}}\right), & \text{from flowering to maturity} \end{cases} \quad (15)$$

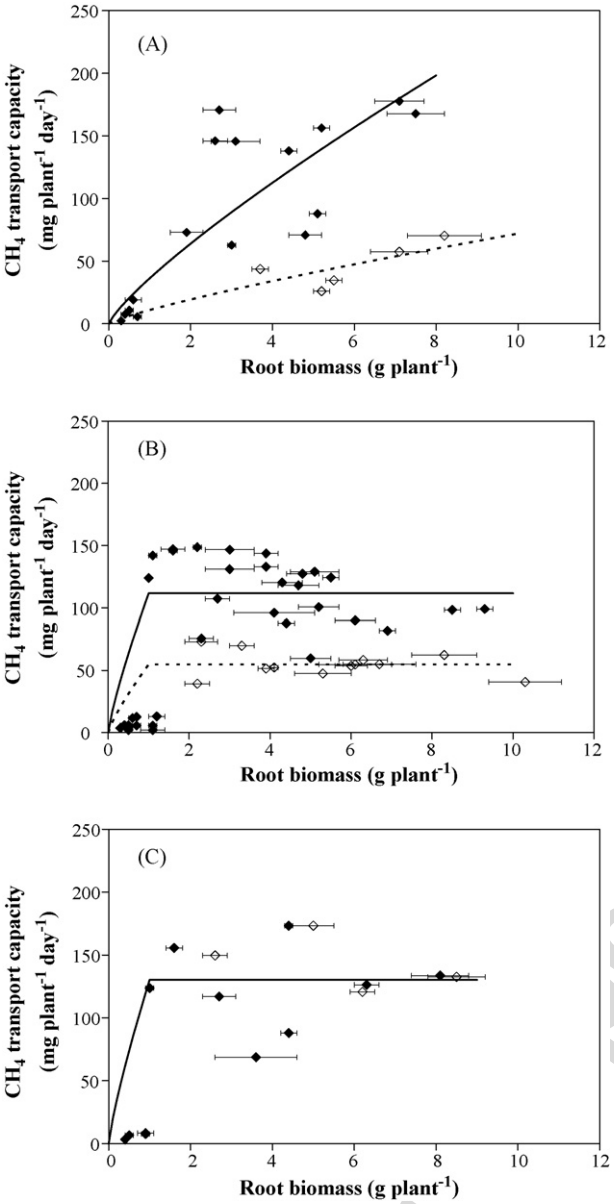

Fig. 4 – Methane transport capacities of (A) tall, (B) dwarf, new plant type, and (C) hybrid cultivars before (closed symbols), and around plant maturity (open symbols), and regression results (solid lines: before maturity; dashed lines: around maturity). Data from Aulakh et al. (2002).

For hybrid cultivars, $\eta = 1$ through the growing season. The default value for MERB in this model was determined to be ~1 g plant^{-1}, based on available experimental data (Fig. 4).

2.6. *Ebullition*

Among the chemical species simulated in this model, methane and hydrogen can escape from sediments into the atmosphere as bubbles. Although the release of methane and hydrogen bubbles from the sediment is an episodic process, here it is assumed that once their concentrations exceed their respective temperature-adjusted solubility, any additional gas production is released instantaneously into the atmosphere through ebullition. The amount of methane that escapes through ebullition is included in the calculation of its total emission.

2.7. *Oxygen release by rice roots*

To allow for aerobic respiration of root cells, herbaceous wetland plants transport oxygen from shoots to roots via the cortical gas-space continuum (Armstrong, 1979), which is also used for the transport of other gases, such as methane, inside rice plants. Usually only a fraction of this oxygen is utilized for root respiration, the rest is released from the roots into the rhizosphere, where it can be used for the oxidation of reduced species, including methane (Gilbert and Frenzel, 1998). Radial oxygen loss (ROL) from rice roots is a highly variable process. No detailed model is currently available to simulate its variation over space and time and for different rice cultivars (Connell et al., 1999; Rubinigg et al., 2002; Colmer, 2003a,b). For a single rice root, a commonly observed feature is that under a reduced environment, ROL decreases with the distance from the root tip (Colmer et al., 1998). At a larger spatial scale, (e.g., one plant), the random vertical distribution of roots supports the argument that the ROL rate is primarily a function of root surface area. For the simulations shown here, an average ROL rate of 0.004 mol m^{-2} day^{-1} was assumed for the early growing season (Rubinigg et al., 2002; Colmer, 2003a,b). In the late growing season, a radial oxygen release rate was assumed to vary accordingly with the methane transport capacity.

2.8. *Temperature dependency of reaction kinetics, diffusivity, and methane transport*

The activity of soil microorganisms increases with temperature up to an optimal value beyond which inactivation of bacterial enzymes and thus decrease in their activities occurs. The temperature dependency of bacterial activities can be described by the Arrhenius equation. If the range of temperature variation is relatively small, the relationship can be approximated by an empirical Q_{10} function, which is defined as the relative increase in reaction rates following a temperature rise of 10 °C (Segers, 1998; Conrad, 2002).

Temperature-dependency of methane production seems to be more variable than that of methane oxidation (Dunfield et al., 1993; Segers, 1998). Q_{10} for methane oxidation was reported to be around 2 (Segers, 1998; Megonigal and Schlesinger, 2002), while Q_{10} for methane production was found to range from 1.5 to 28 with an average of around 4 (Segers, 1998). The stronger and more variable temperature dependency of methane production was attributed to complex interactions of underlying processes (Segers, 1998), such as changes in bacterial activities, functional and structural composition of methanogenic bacteria, and shifts in the carbon and electron flow pathways (Chin and Conrad, 1995; Yao and Conrad, 2000; Wu et al., 2001; Fey and Conrad, 2003). In this model, Q_{10} for methane oxidation and production were assumed to be 2.0 and 4.6, respectively (Segers, 1998; Van Bodegom and Stams, 1999; Walter and Heimann, 2000).

The kinetics of the microbially mediated mineralization of soil organic carbon and most of the redox reactions included

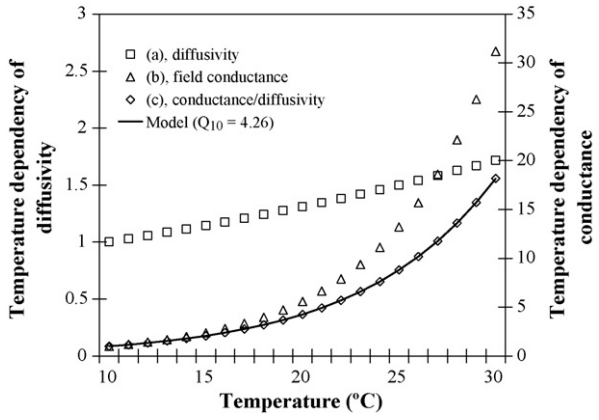

Fig. 5 – Temperature dependency of gaseous diffusivity and plant conductance for methane transport through the aerenchyma system of rice plants. (a) Hosono and Nouchi (1997) and Van Bodegom et al. (2001a,b); (b) Hosono and Nouchi (1997); (c) calculated here.

in this model are also strongly dependent on the soil temperature. Such temperature dependences are also described by the Q_{10} method. For the mineralization of soil organic matter, Q_{10} was reported to be 2.85 (Van Bodegom et al., 2001a,b). Q_{10} values for iron reduction and sulfate reduction were assumed to be 2.4 and 1.6, respectively (Van Bodegom and Stams, 1999). For the decomposition of dead roots as well as other reactions, a Q_{10} value of 2.0 is utilized (Walter and Heimann, 2000; Van Bodegom et al., 2001a,b). The Q_{10} value utilized for the diffusivity of all dissolved species is 1.31 (Hosono and Nouchi, 1997; Segers and Leffelaar, 2001a,b).

Temperature also affects the transport of methane by rice plants (Schutz et al., 1989a,b; Hosono and Nouchi, 1997). There appear to be two independent and multiplicative components in the overall temperature-dependent effect: change in diffusivity of methane, and a physiological change in the rice roots that is not yet well understood (Hosono and Nouchi, 1997). In the laboratory, a Q_{10} value of 1.64, which was independent of the growth stage of rice plants, was reported for the methane transport capacity (Hosono and Nouchi, 1997). Once the temperature dependency of methane diffusion (Q_{10} = 1.31) is separated, the Q_{10} for the temperature-dependent physiological change in the roots was found to be 1.25 (lab) and 4.26 (field) (Hosono and Nouchi, 1997) (Fig. 5). The latter value is comparable to values calculated elsewhere (Schutz et al., 1989a,b). The default value used in this model is thus 4.26.

2.9. *Advective flow induced by rice transpiration*

Rice plants transpire substantial quantities of water from the rhizosphere to the atmosphere and plant transpiration could have important impacts on the biogeochemical processes in wetland systems (Weiss et al., 2006). Although water moves upward inside rice plants, downward advective flow is induced by plant transpiration in the paddy soil and such downward flow could enhance the input of dissolved species, including nutrients and oxygen present in the overlying water (Xu et al., 2004; Xu and Jaffe, 2006). The average transpiration rate in a rice paddy field is around 1000 mm water per growing season and it is usually about one order of magnitude higher than the water loss due to water infiltration (Bethune et al., 2001). In this model, it is assumed that rice transpiration rates are directly related to plant biomass; therefore, the biomass growth function is used to determine the transpiration rate over the growing season while the total amount of water transpired by rice plants remains constant. A dissolved oxygen concentration in the overlying water of 4.0 mg/L coupled with a 1000 mm transpiration rate results in an oxygen input to the soil of 0.125 mol m^{-2} per growing season. This flux of oxygen into the soil results in the direct oxidation of methane or other reduced species, which in turn decrease the methane production, and can reduce the total emission of methane by about 1000 mg m^{-2} per growing season. The transpiration-induced downward flow of water also affects the vertical profiles and fluxes of the other dissolved species that either directly or indirectly affect methane production in the soil, as well as retards the upward diffusion of methane towards the soil surface.

3. Model evaluation

The coupled partial differential equations (PDEs) for the dissolved and solid species are solved numerically through an iterative scheme following the discretization via second-order accurate finite difference approximation (Smith and Jaffe, 1998; Park and Jaffe, 1999). The reaction kinetics are described as either a dual-species Monod or second order kinetics, see for example (Jaffe et al., 2002) for a detailed description.

Thermodynamic theory and experimental evidence indicate that terminal electron acceptors in the sediment are utilized in a sequence that corresponds to the energy yield from the oxidation of organic substrates (Stumm and Morgan, 1996). Methanogenesis in rice paddy soils, therefore, could be inhibited by the presence of energetically more favorable terminal electron acceptors, such as oxygen, nitrate, Mn(IV), Fe(III) and sulfate. In this model, an indicator function strategy is adopted, which has been applied successfully in the modeling of the sequential utilization of electron acceptors in sediments (Park and Jaffe, 1996; Van Cappellen and Wang, 1996; Smith and Jaffe, 1998) and rice paddy soils (Matthews et al., 2000a,b; Van Bodegom et al., 2001a,b). With this indicator function scheme, when the concentration of one terminal electron acceptor falls below its cutoff value (listed in Table 1),

Table 1 – Cutoff values for alternative terminal electron acceptors below which the next most energetically favorable electron accepting process is allowed to proceed

Species	Cutoff value (μM)
O_2	0.5[a]
NO_3^-	5[b]
Mn(IV)	0.9[a]
Fe(III)	8[a,b]
SO_4^{2-}	1000[b]

[a] Smith and Jaffe (1998).
[b] Van Cappellen and Wang (1996).

Table 2 – General model parameters

Parameter	Description	Value	Unit
X_L	Maximum depth of soil	0.5	m
ET	Evapotranspiration rate	1000	mm/growing season
ϕ	Porosity	0.3	
ρ	Bulk density	1.3	kg/L
D_{O_2}	Molecular diffusion coefficient of oxygen in soil solution	9.8×10^{-1}	m^2/day
D_{CH_4}	Molecular diffusion coefficient of methane in soil solution	1.20	m^2/day
D_{H_2}	Molecular diffusion coefficient of hydrogen in soil solution	4.61	m^2/day
D_{Ac}	Molecular diffusion coefficient of acetate in soil solution	5.81×10^{-1}	m^2/day
$D_{Fe(II)}$	Molecular diffusion coefficient of Fe(II) in soil solution	6.11×10^{-1}	m^2/day
D_M	Typical molecular diffusion coefficient of dissolved species	1.10	m^2/day
$Q_{10,D}$	Q_{10} for diffusion coefficient	1.31	
T_f	Relative time of rice plant flowering in growing season	0.6	
T_d	Relative time in growing season when root dieback starts	0.67	
L_{rw}	Thickness of rice root epidermis	0.025	mm
P_{r,CH_4}	Partial pressure of methane in the aerenchyma of rice plant	0	atm
P_{r,H_2}	Partial pressure of hydrogen in the aerenchyma of rice plant	0	atm
α_L	Coefficient to calculate dispersion coefficient (when multiplied by velocity, dispersion coefficient is obtained)	0.5	

the next most energetically favorable electron accepting process is allowed to proceed. The order of the sequential utilization of electron acceptors is: oxygen, nitrate, Mn(IV), Fe(III), and sulfate. For instance, the utilization of nitrate does not begin until the concentration of oxygen falls below its cutoff value listed in Table 1. When oxygen concentration is below its cutoff value, both oxygen and nitrate are used simultaneously. Competition for substrate between sulfate reducers and methanogenic bacteria that has been observed experimentally is reflected by the relatively high cutoff values of sulfate (Roy et al., 1997) (i.e., methanogenesis can proceed in the presence of significant amounts of sulfate). Required model and reaction kinetic parameters are included in Tables 2 and 3, respectively. Each row in Table 3 represents one specific reaction term and the chemical species included in this model are coupled through these reactions terms.

The performance of the model is tested against methane emission measurements obtained from irrigated rice fields

Table 3 – Reaction kinetic parameters used in the simulations

Reaction	Type of kinetics	Parameters
Oxygen–carbon	Dual monod	$V_{max} = 1.30 \times 10^{-3}$ (a), $K_{s,carbon} = 1.56 \times 10^{-3}$ (b), $K_{s,O_2} = 1.07 \times 10^{-5}$ (b)
Oxygen–H_2	Dual monod	$V_{max} = 1.30 \times 10^{-3}$ (c), $K_{s,H_2} = 1.00 \times 10^{-7}$ (j), $K_{s,O_2} = 1.07 \times 10^{-5}$ (c)
Oxygen–sulfide	Second-order	$k = 5.48 \times 10^{2}\ M^{-1}\ day^{-1}$ (d)
Oxygen–Mn(II)	Second-order	$k = 1.26 \times 10^{-2}\ M^{-1}\ day^{-1}$ (d)
Oxygen–ammonium	Dual monod	$V_{max} = 8.20 \times 10^{-2}$ (e), $K_{s,NH_4^+} = 5.56 \times 10^{-3}$ (f), $K_{s,O_2} = 1.07 \times 10^{-5}$ (c)
Oxygen–Fe(II)	Second-order	$k = 2.97 \times 10^{4}\ M^{-1}\ day^{-1}$ (b)
Oxygen–methane	Dual monod	$V_{max} = 2.07 \times 10^{-1}$ (g), $K_{s,CH_4} = 3.07 \times 10^{-5}$ (b), $K_{s,O_2} = 4.70 \times 10^{-6}$ (b)
Nitrate–carbon	Dual monod	$V_{max} = 1.30 \times 10^{-3}$ (h), $K_{s,carbon} = 9.0 \times 10^{-5}$ (h), $K_{s,NO_3^-} = 4.2 \times 10^{-4}$ (h)
Nitrate–H_2	Dual monod	$V_{max} = 1.30 \times 10^{-3}$ (h), $K_{s,H_2} = 1.0 \times 10^{-7}$ (h), $K_{s,NO_3^-} = 4.2 \times 10^{-4}$ (h)
Nitrate–sulfide	Dual monod	$V_{max} = 7.35 \times 10^{-4}$ (h), $K_{s,S^{2-}} = 1.68 \times 10^{-3}$ (h), $K_{s,NO_3^-} = 1.75 \times 10^{-3}$ (h)
Mn(IV)–carbon	Dual monod	$V_{max} = 2.74 \times 10^{-5}$ (d), $K_{s,carbon} = 9.0 \times 10^{-5}$ (a), $K_{s,Mn(IV)} = 2 \times 10^{-6}$ (d)
Mn(IV)–H_2	Dual monod	$V_{max} = 2.74 \times 10^{-5}$ (i), $K_{s,H_2} = 1.0 \times 10^{-7}$ (j), $K_{s,Mn(IV)} = 2 \times 10^{-6}$ (i)
Mn(IV)–sulfide	Second-order	$k = 2.19 \times 10^{3}\ M^{-1}\ day^{-1}$ (d)
Mn(IV)–Fe(II)	Second-order	$k = 27.4\ M^{-1}\ day^{-1}$ (d)
Fe(III)–carbon	Dual monod	$V_{max} = 5.40 \times 10^{-3}$ (h), $K_{s,carbon} = 2.3 \times 10^{-4}$ (h), $K_{s,Fe(III)} = 6.1 \times 10^{-2}$ (h)
Fe(III)–H_2	Dual monod	$V_{max} = 5.20 \times 10^{-3}$ (b), $K_{s,H_2} = 2.2 \times 10^{-4}$ (h), $K_{s,Fe(III)} = 6.1 \times 10^{-2}$ (h)
Fe(III)–sulfide	Second-order	$k = 2.74\ M^{-1}\ day^{-1}$ (d)
Sulfate–carbon	Dual monod	$V_{max} = 8.63 \times 10^{-5}$ (h), $K_{s,carbon} = 7.90 \times 10^{-4}$ (h), $K_{s,SO_4^{2-}} = 2.30 \times 10^{-4}$ (h)
Sulfate–H_2	Dual monod	$V_{max} = 8.00 \times 10^{-6}$ (h), $K_{s,H_2} = 2.87 \times 10^{-6}$ (h), $K_{s,SO_4^{2-}} = 2.30 \times 10^{-4}$ (h)
Sulfate–methane	Second-order	$k = 27.4\ M^{-1}\ day^{-1}$ (d)
Methanogenesis-acetate	Monod	$V_{max} = 2.26$ (k) or 3.30 (l) $\times 10^{-4}$ (m), $K_{s,carbon} = 2.56 \times 10^{-3}$ (h)
Methanogenesis-H_2	Monod	$V_{max} = 6.56 \times 10^{-4}$ (b), $K_{s,H_2} = 1.33 \times 10^{-5}$ (b)

(a) Same as nitrate–carbon reaction, (b) from Van Bodegom et al. (2001a,b), (c) same as oxygen–carbon reaction, (d) from Smith and Jaffe (1998), (e) from Wang et al. (2003), (f) from Wynn and Liehr (2001), (g) from Arah and Stephen (1998), (h) from Van Bodegom and Scholten (2001), (i) same as Mn(IV)–carbon reaction, (j) same as nitrate–H_2 reaction, (k) for field site in Chongqing, (l) for field site in Sichuan, and (m) from Segers (1998).

Table 4 – Initial and boundary conditions for the simulations of the Chongqing site

Species	Initial (mol L^{-1})	Top		Bottom	
		Type	Value	Type	Value
O_2	1.25×10^{-4}	Concentration	1.25×10^{-4}	Gradient	0
Fe(III)[a]	5.39×10^{-2}	Gradient	0	Gradient	0
Fe(II)[b]	1.26×10^{-1}	Concentration	0	Gradient	0
Mn(IV)[a]	3.51×10^{-4}	Gradient	0	Gradient	0
Mn(II)[b]	8.19×10^{-4}	Concentration	0	Gradient	0
Solid organic	–[c]	Gradient	0	Gradient	0

[a] Initial concentrations were zero for 1998.
[b] Initial concentrations were zero for 1999.
[c] Profile of solid organic carbon was provided as initial conditions.

located in Chongqing (Cai et al., 2003) and Sichuan (Khalil et al., 1998a,b), China. Methane production rates are usually a function of the density, structural, and functional composition and activity of methanogenic bacteria. No direct measurements of the maximum specific methane production rates at either testing sites were conducted. Therefore, the maximum methane production rate measured for soil samples collected from Hangzhou, China is taken and only slight adjustments are allowed at each testing site to achieve an optimal match between model output and field observations (Wang et al., 1999). At each testing site, the maximum methane production rate is assumed to be constant during the growing season, since the density of both hydrogenotrophic and acetotrophic methanogens in rice paddy soils was found to be fairly stable during the growing season (Schutz et al., 1989a,b).

Organic matter content in surface soil at the Chongqing site was determined to be 1.3% (Z. Cai, personal communication). A dwarf rice cultivar was grown at the Chongqing site and methane emission rates during the growing season were measured. Similar agricultural practices were performed throughout the duration of the field experiment. Briefly, rice fields were flooded in the winter (except for 1998, due to the dry weather, the fields were flooded 1 week before transplanting), and in May rice seedlings were transplanted at a density of about 30 plants m^{-2} (Z. Cai, personal communication), after about 100 days, the grain was harvested. Approximately two measurements of methane fluxes were made every week, and the soil temperature at a depth of 5 cm was recorded.

Methane emission rates were also measured at Tuzu (located in Sichuan province, China) where hybrid rice cultivars were grown (Khalil et al., 1998a,b). At this site, an attempt was made to account for heterogeneity in rice emission kinetics at relative small spatial (~100 m) and temporal (~1 day) scales by taking up to 24 measurements each day. Plant density was reported to be 30 plants m^{-2} while organic carbon content of surface soil was reported to be 1.57% (Khalil et al., 1998a,b).

Model input data include initial concentrations of soil organic matter and electron acceptors (oxygen, nitrate, manganese, iron and sulfate), maximum root biomass and maximum effective root biomass, which can be estimated from rice yield data, and soil temperature. The initial and boundary conditions used in these simulations are listed in Tables 4 and 5, respectively. Plant growth data are listed in Table 6. Rice yield values were used to estimate maximum root biomass and maximum effective root biomass (MERB). In 1998, the Chongqing field was drained during the winter and only flooded 1 week before transplanting. In the simulations accounting for a significant drainage time it was assumed that the reduced iron and manganese were completely converted to Fe(III) and Mn(IV), respectively, after drainage. Following field flooding, Mn(IV) and Fe(III) were sequentially utilized as electron acceptors. Field drainage before transplanting, therefore, could reduce methane emission rates during early growing season since the onset of methane production is delayed until Mn(IV) and Fe(III) are consumed. In 1999, the Chongqing field remained flooded throughout the winter, and iron and manganese are assumed to exist in their reduced forms as Fe(II) and Mn(II). For this case a simulation was initiated to simulate the dynamics 1 week before transplanting. For the Sichuan site, flooding of rice fields is assumed to have started 1 week before transplanting; prior to the flooding, the

Table 5 – Initial and boundary conditions for the simulations of the Sichuan site

Species	Initial (mol L^{-1})	Top		Bottom	
		Type	Value	Type	Value
O_2	1.25×10^{-4}	Concentration	1.25×10^{-4}	Gradient	0
Fe(III)	2.29×10^{-2}	Gradient	0	Gradient	0
Mn(IV)	1.10×10^{-3}	Gradient	0	Gradient	0
Solid organic	–[a]	Gradient	0	Gradient	0

[a] The vertical profile of solid organic carbon was provided as initial conditions.

Table 6 – Length of growing season, annual rice yield, maximum root biomass, and maximum effective root biomass (MERB) for the testing sites located in Chongqing and Sichuan (China), respectively

	Site					
	Chongqing		Sichuan			
	1998	1999	1988	1989	1992	1993
Length of growing season (days)	100	98	120	128	108	106
Yield (t ha^{-1})	7.03	7.90	5.25	4.875	6.72	5.43
Maximum root biomass (g plant^{-1})	6.49	7.29	4.85	4.5	6.2	5.01
MERB (g plant^{-1})	1.08	1.22	0.81	0.75	1.03	0.84

Maximum root biomass and MERB are assumed to be proportional to rice yield, and when rice yield is 6.5 t/ha, maximum root biomass and MERB are 6.00 and 1.0 g plant^{-1}, respectively.

soil was aerobic and the iron and manganese were in the oxidized forms.

Example of comparisons between model outputs and field measurements are illustrated in Fig. 6. Overall, the model captures the main features of methane flux dynamics over the growing seasons well, including the temporal variations at time scales from one to several days. The inclusion of the dynamics of alternative electron acceptors and their inhibitive effects on methane production allows for the prediction of the time at which methane emissions are initiated after flooding: methane production does not start until the bioavailable Fe(III) and Mn(IV) are depleted. This will also enable an analysis of the impacts of mineral fertilizer application and field drainage on methane production and hence the methane emission over a growing season. Consistent with field observations, methane emission due to ebullition accounts for about 10% of total methane fluxes (Butterbach-Bahl et al., 1997; Hosono and Nouchi, 1997).

4. Discussion

This section examines the effects of root oxygen release, plant transpiration, cultivar selection, changes in temperature, application of mineral fertilizer, and field drainage on seasonal methane fluxes. These processes and parameters are selected based on their significance on methane fluxes revealed by the results of preliminary tests and for their relevance to methane emission mitigation efforts. For the purpose of conciseness, with a few exceptions, only results obtained during 1999 from Chongqing and in 1988 from Sichuan are used in the discussion.

4.1. *Radial oxygen release*

Based on the simulations, about 6% of the methane produced in the soil is oxidized by oxygen released from the roots at both testing sites. Similarly if the average oxygen release rate is doubled, 6% less methane is emitted at both sites. The difference in methane fluxes under different oxygen release scenarios is more significant during the late growing season. This is due to the presence of large amounts of root biomass during that time, and the total amount of oxygen released by roots is primarily determined by root surface area.

4.2. *Plant transpiration*

Water infiltration, induced by plant transpiration, impacts methane emission in various ways. First, oxygen transport from the overlying water into the soil is enhanced. Second, an enhanced infiltration flow will decrease the upward diffusive flux of methane, and lead to the redistribution of various dissolved species such as organic carbon. The simulations show that the net effect of plant transpiration is a slight decrease (4%) in methane emission. This is mainly because infiltration induced by plant transpiration leads to deeper penetration of dissolved oxygen present in the overlying water, which in turn could inhibit methane production and also oxidize methane. If fertilizers containing nitrate or sulfate are applied to the surface layer of the soil, plant transpiration could enhance their downward transport and thus suppress methane production activities in the bottom layers.

4.3. *Rice cultivars*

Experimental data have shown that different rice cultivars have remarkably different methane transport capacities and seasonal patterns of that transport capacity (Fig. 4) (Aulakh et al., 2002). Therefore, selection of rice cultivars that are less efficient in transporting methane could be an option for reducing methane emissions. Inclusion of the detailed plant mediated methane transport term enables us to examine the effects of rice cultivars on overall methane emission. The simulations reveal small (<4%) differences in methane emission rates between fields planted with either dwarf/NPT or hybrid cultivars (Fig. 7). Tall cultivars could reduce seasonal methane emission rate by 12% (Sichuan site) to 15% (Chongqing site). At the seedling stage, tall cultivars are significantly less efficient in mediating the transport of methane: 28% as efficient as hybrid cultivars and 35% as efficient as dwarf/NPT cultivars. At this stage, however, a higher fraction of produced methane is emitted through the ebullition pathway. After the seedling stage, the methane transport capacity by dwarf/NPT and hybrid cultivars levels off, while the methane transport capacity by tall cultivars continuously increases with the growth of roots (Fig. 4). This suggests that as low conductive rice cultivars may represent a feasible mitigation option for methane emission from rice paddy fields, evaluation and assessment should be based on measurements of cultivar-dependent methane

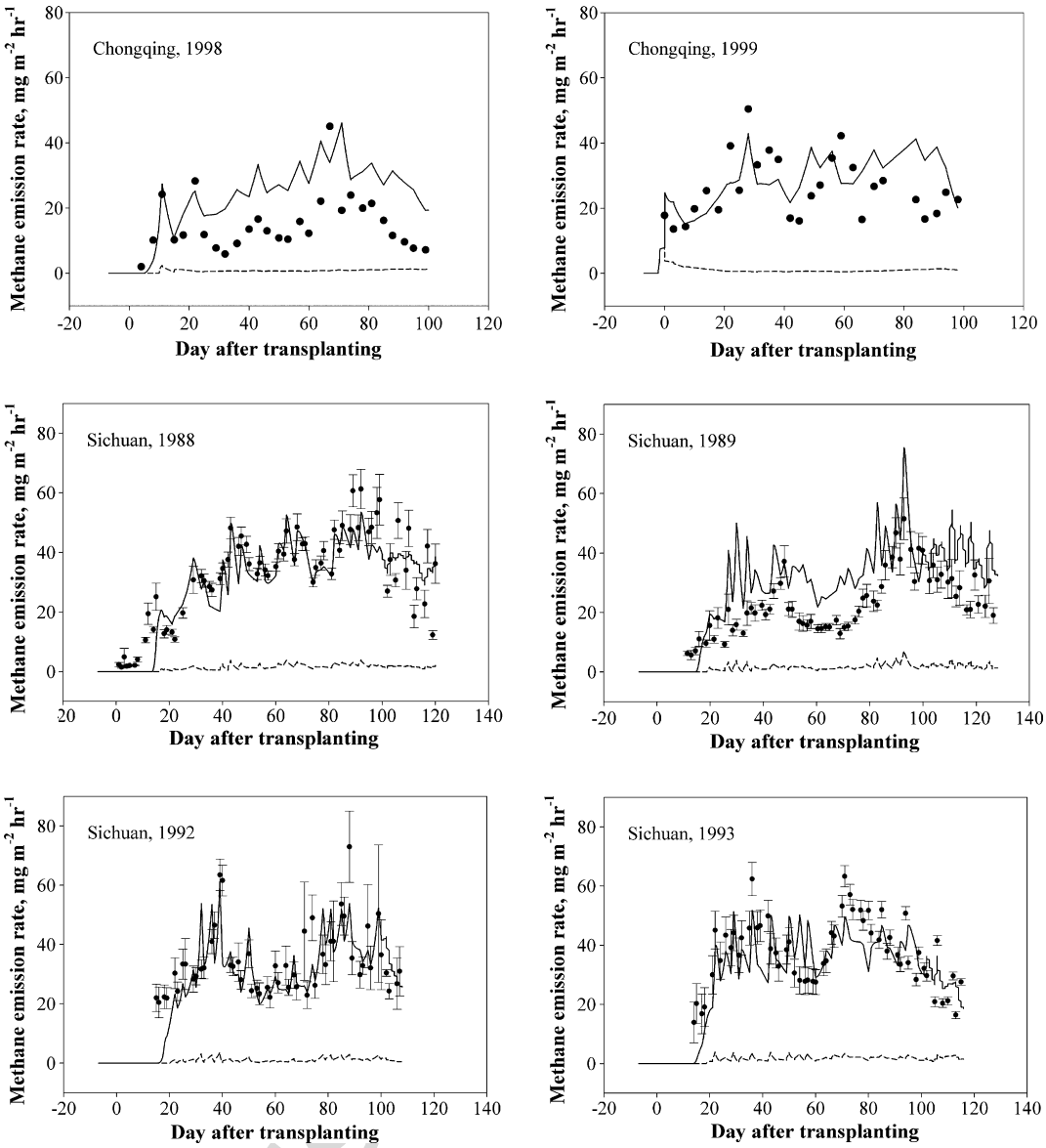

Fig. 6 – Methane emission rates during the growing seasons of 1998–1999 at rice fields located in Chongqing, China (Cai et al., 2003) and during growing seasons of 1988–1989, 1992–1993 at rice fields located in Sichuan, China (Khalil et al., 1998a,b). Symbols are field measurements. Solid lines represent model predictions of total methane emission rates and dotted lines are predicted methane emission rates due to ebullition.

transport capacities over the whole growing season. The simulation results are consistent with previous report that showed small variation in methane fluxes among fields planted with different rice cultivars (Khalil et al., 1998a,b).

4.4. *Temperature*

Temperature controls most of the processes included in the model, resulting in complex relationships between temperature and methane emissions. The effects of temperature on the seasonal variation in methane fluxes and on the overall emission of methane from rice paddy systems are examined here.

Two maxima of methane fluxes during the growing season were observed at the Sichuan site (Fig. 6) and this phenomenon has been attributed to the supply of nutrients in the soil, to root exudates, or to temperature variations (Khalil et al., 1998a,b). Results from 1992 from the Sichuan site are used here, as an example, to show the significance of the temperature dependency of methane production and transport for the bimodal pattern in methane fluxes (Fig. 8). When methane production rates and plant-mediated methane transport are independent of soil temperature, the bimodal pattern almost disappears in the model predictions. This suggests that temperature, and more specifically, the effect of temperature on methane production and transport, is the major factor controlling the observed bimodal pattern of methane flux at the Sichuan site.

Since the late 19th century, the global mean surface air temperature has increased by 0.3–0.6 °C (IPCC, 1995a,b). As

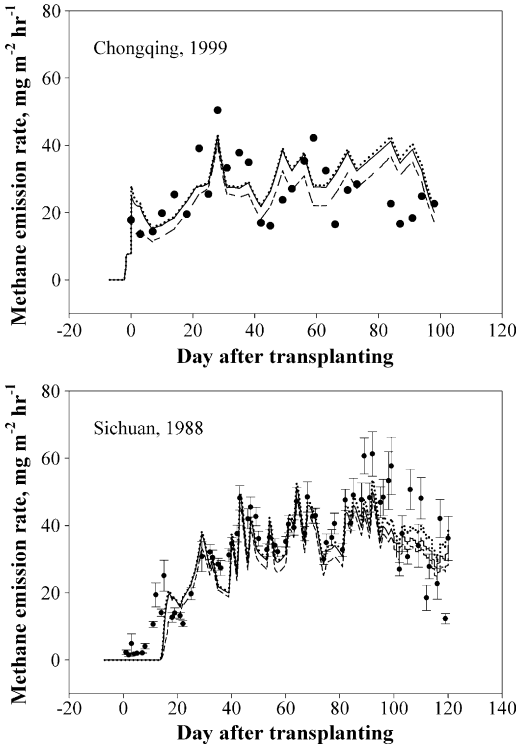

Fig. 7 – Methane emission rates for different rice cultivars. Symbols represent field measurements, dashed lines represent traditional tall cultivars, solid lines represent dwarf and new plant type cultivars, and dotted lines represent hybrid cultivars.

methane is one of the major greenhouse gases responsible for such a rise in temperature a potential positive feedback exists. Variations in temperature may change both the absolute and relative sizes of methane sources and sinks and thus its concentration in the atmosphere and contribution to global radiative forcing.

The simulations show that a slight increase in soil temperature enhances the methane emission from rice paddy soils significantly. At the Chongqing site, an increase of soil temperature by 1 °C, 2 °C, and 3 °C, respectively, results in a 15%, 32% and 52% increase in seasonal methane emission rates. Similarly, total methane emission over the growing season from the Sichuan site increases by 9%, 29%, and 51% if soil temperature rises by 1 °C, 2 °C, and 3 °C, respectively. Such predictions are consistent with the historical record of temperature and atmospheric methane concentration from more than 400,000 years ago until the pre-industrial period (Wuebbles and Hayhoe, 2002) and by the results from the recent meta-analysis of northern wetlands (Christensen et al., 2003). Elevated atmospheric methane levels will likely enhance temperature increases. If elevated temperature persists over long periods of time, the ultimate limit of methane emission from rice paddies would then be the availability of organic substrates. The long-term changes in the soil organic carbon pool are not simulated here, and should be included for the assessment of changes in methane emission due to either long-term cultivation practices or climate change.

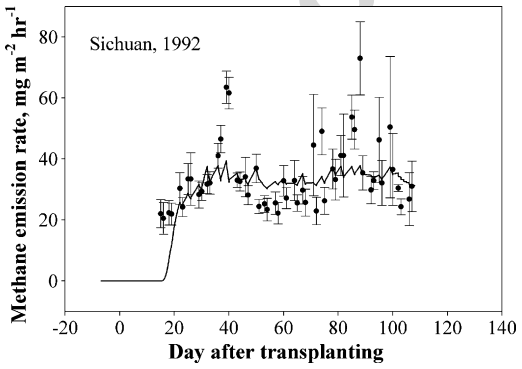

Fig. 8 – Effects of temperature dependency of the plant conductance and methane production on methane flux. Symbols represent field measurements and line is predicted flux (methane production and plant conductance are independent on temperature).

4.5. *Effects of nitrate fertilizer application*

Application of nitrogen fertilizer is a common practice in rice cropping. The most commonly applied nitrogen fertilizer in rice paddy fields is reduced nitrogen such as ammonium and urea. It has been shown, however, that rice can grow as well or better with the application of nitrate, especially when nitrate is mixed with ammonium or urea (Fan et al., 2005; Li et al., 2006). The presence of nitrate could inhibit methane production and thus reduce methane emission rate. For the Chongqing site, 273 kg/ha of urea was applied, which was equivalent to 127.4 kgN/ha. Both compound fertilizer (containing 13% of nitrogen) as well as urea were applied at the Sichuan site, with an average application rate of 64 kgN/ha. To examine the effects of nitrate fertilizer application on methane emission, simulations were conducted assuming that half of the nitrogen fertilizers applied at each site was nitrate instead of urea. Soil depth of fertilizer application was assumed to be the top 30 cm. Experiments conducted with a variety of Chinese rice cultivars suggested that there was no significant difference in rice plant growth when 50% of ammonium-type of fertilizer was replaced with nitrate (Fan et al., 2005; Li et al., 2006). Therefore, no change was made in the model in terms of plant growth dynamics and root biomass.

Compared with the default case, the application of nitrate fertilizer leads to a 6% (Chongqing site) and 3% (Sichuan site) decrease in cumulative seasonal methane fluxes (Fig. 9). This is primarily due to the inhibitory effects of nitrate on methanogenesis. Simulation results also showed that, once flooded, nitrate could be reduced to ammonium very quickly. Although rice plants may experience slower growth when nitrate is used as the sole nitrogen source, a mixture of nitrate and ammonium can be created soon after the application of nitrate fertilizer. Therefore, although experiments conducted under aerobic conditions suggested that nitrate, as the sole nitrogen source, could lead to slow growth in rice plants, the application of nitrate-only fertilizer may not have a significant impact on rice growth in flooded rice paddy fields. The reduction of seasonal methane emission could be more than 10% if nitrate was applied as the only nitrogen fertilizer at the Chongqing site. A major disadvantage of nitrate application as a strategy

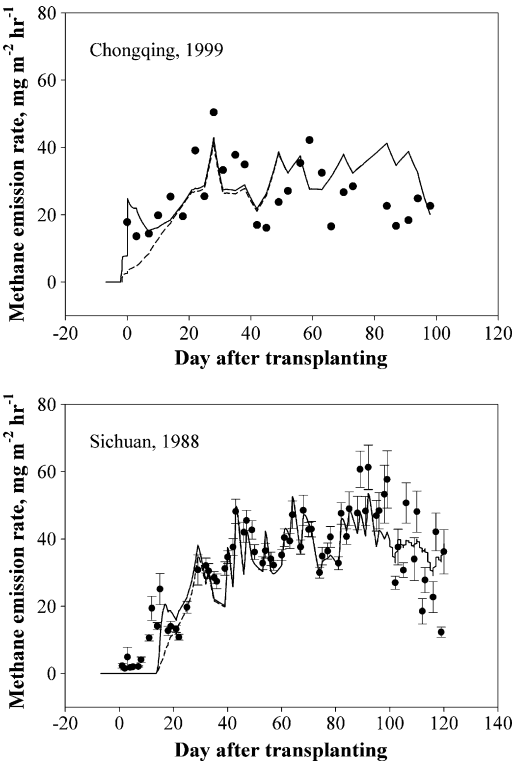

Fig. 9 – Effects of the application of nitrate fertilizer on methane fluxes. Symbols represent field measurements, solid lines represent default model predictions, and dashed lines represent simulation results assuming that half of the nitrogen fertilizer was applied in the form of nitrate.

to reduce methane emissions is that emissions of N_2O, which is also a greenhouse gas, will become significant when the soil redox potential is high (Yu and Patrick, 2003). Emission of NO, a precursor for the production of O_3, a regional air pollutant, may also increase.

4.6. *Effects of field drainage*

For the Chongqing site, prolonged flooding of the field before transplanting led to the complete reduction of iron and manganese. If the field was drained several weeks before transplanting, the iron and manganese would be oxidized to Fe(III) (1620 mg/kg) and Mn(IV) (10 mg/kg). Since reductions of Mn(IV) and Fe(III) are more energetically favorable than methanogenesis, methanogenesis would be suppressed in the early growing season during the reduction of Fe(III) and Mn(IV). For the year of 1999, simulation results show that the drainage prior to planting would result in an 8% decrease in seasonal methane flux.

Drainage was carried out before transplanting for the Sichuan site. The effects of iron and manganese on methane emission can be examined by assuming a prolonged flooding prior to the growing season. According to this model, if the site had not been drained and both iron (690 mg/kg) and manganese (32.5 mg/kg) existed in their reduced forms at the beginning of the growing season, seasonal methane flux would increase by 10%.

Mid-season drainage of rice fields is becoming an increasingly popular practice in China, the largest rice producer in the world (Jiao et al., 2006; Li et al., 2002a,b; Yan et al., 2005). The primary motivation behind mid-season drainage is water conservation. It has also been reported the mid-season drainage could improve rice yields (Li et al., 2002a,b). Once drained, the penetration of oxygen can significantly suppress methane production directly and indirectly through converting reduced iron and manganese to Fe(III) and Mn(IV), respectively. Model simulations were performed to quantify the impact of mid-season drainage on methane emission.

In these mid-season drainage simulations, it was assumed that the rice field was drained around the middle of the growing season for 1 week (Jiao et al., 2006). Once the field was drained, methane production and emission usually was negligible (Zou et al., 2005) and reduced iron and manganese were oxidized. Results showed that 1-week drainage at the middle of the growing season could significantly reduce seasonal methane emission: 22% for the Chongqing site and 23% for the Sichuan site (Fig. 10). Combined, pre-season and mid-season drainage can reduce seasonal methane emission by about 30%. Because both reduced iron and manganese are converted to their oxidized forms, methane production and emission are usually inhibited after the re-flooding of rice fields (Fig. 10). Since field drainage can simultaneously conserve water, improve rice yield and significantly reduce methane emission, it deserve further promotion through both policy and economical tools.

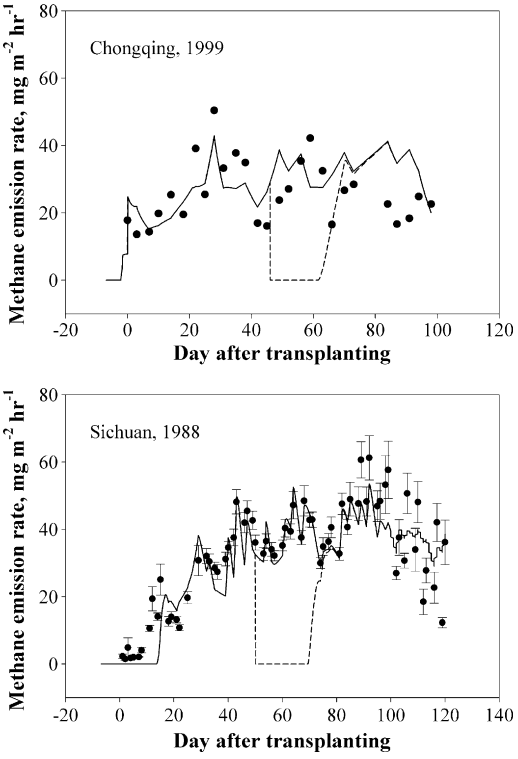

Fig. 10 – Effects of mid-season drainage on methane emission. Symbols represent field measurements, solid lines represent default model predictions without mid-season drainage, and dashed lines represent simulation results with a 1-week mid-season drainage.

5. Conclusions

The one-dimensional, process-based methane emission model for rice paddy systems presented here, attempts to include all of the major processes relevant to methane production, oxidation and emission. Some of the processes included here, such as the cultivar-dependent methane transport capacity, vertical flow induced the plant transpiration, and the temperature dependency of rice-mediated methane transport capacity, have not been considered and evaluated together in previous methane emission models. Comparison of model simulation results and 6 years of field observations shows that the model is capable of capturing the temporal variations of methane emissions over a growing season. The impacts of a variety of environmental and agricultural conditions on methane fluxes are simulated and the potential of many mitigation options explored. Plant transpiration is found to slightly decrease methane emission through the downward transport of dissolved oxygen. Under conditions in the two testing sites, tall rice cultivars are found to have noticeable effects (12–15% decrease) on the overall methane emissions. The model predictions are consistent with field observations in terms of the impact of temperature change on methane emissions. The application of nitrate fertilizers and field drainage can reduce methane emissions by 3–10%. Pre-season and mid-season drainage could remarkably reduce methane emission at both testing sites and represent a promising mitigation option. The model will be applied to rice fields in China, the largest rice producer in the world, to establish methane emission inventories and to evaluate the feasibility and cost-effectiveness of various methane emission mitigation options in various regions.

Acknowledgements

Research by S. Xu was supported by the Princeton Environmental Institute—Science, Technology and Environmental Policy (PEI-STEP) Fellowship Program. We are grateful to Z. Cai, S. Singh, M. Aulakh, S. Wassmann, R. Rennenberg, and M. Wissuwa for providing data and insights on their experimental work. The constructive comments provided by Dr. Sven Jørgensen and an anonymous reviewer, which led to the improvement of this manuscript are also gratefully acknowledged.

REFERENCES

Arah, J.R.M., Kirk, G.J.D., 2000. Modeling rice plant-mediated methane emission. Nutr. Cycl. Agroecosyst. 58, 221–230.

Arah, J.R.M., Stephen, K.D., 1998. A model of the processes leading to methane emission from peatland. Atmos. Environ. 32, 3257–3264.

Armstrong, W., 1979. Aeration in higher plants. Adv. Bot. Res. 7, 226–333.

Aulakh, M.S., Bodenbender, J., Wassmann, R., Rennenberg, H., 2000a. Methane transport capacity of rice plants. I. Influence of methane concentration and growth stage analyzed with an automated measuring system. Nutr. Cycl. Agroecosyst. 58, 357–366.

Aulakh, M.S., Bodenbender, J., Wassmann, R., Rennenberg, H., 2000b. Methane transport capacity of rice plants. II. Variations among different rice cultivars and relationship with morphological characteristics. Nutr. Cycl. Agroecosyst. 58, 367–375.

Aulakh, M.S., Wassmann, R., Bueno, C., Kreuzwieser, J., Rennenberg, H., 2001a. Characterization of root exudates at different growth stages of ten rice (*Oryza sativa* L.) cultivars. Plant Biol. 3, 139–148.

Aulakh, M.S., Wassmann, R., Bueno, C., Rennenberg, H., 2001b. Impact of root exudates of different cultivars and plant development stages of rice (*Oryza sativa* L.) on methane production in a paddy soil. Plant Soil 230, 77–86.

Aulakh, M.S., Wassmann, R., Rennenberg, H., 2001c. Methane emissions from rice fields—quantification, mechanisms, role of management, and mitigation options. Adv. Agron. 70, 193–260.

Aulakh, M.S., Wassmann, R., Rennenberg, H., 2002. Methane transport capacity of twenty-two rice cultivars from five major Asian rice-growing countries. Agric. Ecosyst. Environ. 91, 59–71.

Bachelet, D., Kern, J., Tolg, M., 1995. Balancing the rice carbon budget in china using spatially-distributed data. Ecol. Model. 79, 167–177.

Bethune, M., Austin, N., Maher, S., 2001. Quantifying the water budget of irrigated rice in the Shepparton irrigation region, Australia. Irrig. Sci. 20, 99–105.

Bodelier, P.L., Roslev, P., Henckel, T., Frenzel, P., 2000. Stimulation by ammonium-based fertilizers of methane oxidation in soil around rice roots. Nature 403, 421–424.

Butterbach-Bahl, K., Papen, H., Rennenberg, H., 1997. Impact of gas transport through rice cultivars on methane emission from rice paddy fields. Plant Cell Environ. 20, 1175–1183.

Cai, Z.C., Tsuruta, H., Gao, M., Xu, H., Wei, C.F., 2003. Options for mitigating methane emission from a permanently flooded rice field. Global Change Biol. 9, 37–45.

Cao, M.K., Dent, J.B., Heal, O.W., 1995. Modeling methane emissions from rice paddies. Global Biogeochem. Cycles 9, 183–195.

Cao, M.K., Gregson, K., Marshall, S., 1998. Global methane emission from wetlands and its sensitivity to climate change. Atmos. Environ. 32, 3293–3299.

Chin, K.J., Conrad, R., 1995. Intermediary metabolism in methanogenic paddy soil and the influence of temperature. FEMS Microbiol. Ecol. 18, 85–102.

Christensen, T.R., Ekberg, A., Strom, L., Mastepanov, M., Panikov, N., Mats, O., Svensson, B.H., Nykanen, H., Martikainen, P.J., Oskarsson, H., 2003. Factors controlling large scale variations in methane emissions from wetlands. Geophys. Res. Lett. 30.

Cicerone, R.J., Shetter, J.D., 1981. Sources of atmospheric methane—measurements in rice paddies and a discussion. J. Geophys. Res. Oceans Atmos. 86, 7203–7209.

Colmer, T.D., 2003a. Aerenchyma and an inducible barrier to radial oxygen loss facilitate root aeration in upland, paddy and deep-water rice (*Oryza sativa* L.). Ann. Bot. 91, 301–309.

Colmer, T.D., 2003b. Long-distance transport of gases in plants: a perspective on internal aeration and radial oxygen loss from roots. Plant Cell Environ. 26, 17–36.

Colmer, T.D., Gibberd, M.R., Wiengweera, A., Tinh, T.K., 1998. The barrier to radial oxygen loss from roots of rice (*Oryza sativa* L.) is induced by growth in stagnant solution. J. Exp. Bot. 49, 1431–1436.

Connell, E.L., Colmer, T.D., Walker, D.I., 1999. Radial oxygen loss from intact roots of *Halophila ovalis* as a function of distance behind the root tip and shoot illumination. Aquat. Bot. 63, 219–228.

Conrad, R., 1999. Contribution of hydrogen to methane production and control of hydrogen concentrations in

methanogenic soils and sediments. FEMS Microbiol. Ecol. 28, 193–202.
Conrad, R., 2002. Control of microbial methane production in wetland rice fields. Nutr. Cycl. Agroecosyst. 64, 59–69.
Conrad, R., Klose, M., 2000. Selective inhibition of reactions involved in methanogenesis and fatty acid production on rice roots. FEMS Microbiol. Ecol. 34, 27–34.
Dunfield, P., Knowles, R., Dumont, R., Moore, T.R., 1993. Methane production and consumption in temperate and sub-Arctic peat soils—response to temperature and pH. Soil Biol. Biochem. 25, 321–326.
Fan, X.R., Shen, Q.R., Ma, Z.Q., Zhu, H.L., Yin, X.M., Miller, A.J., 2005. A comparison of nitrate transport in four different rice (*Oryza sativa* L.) cultivars. Sci. China C: Life Sci. 48, 897–911.
Fey, A., Conrad, R., 2003. Effect of temperature on the rate limiting step in the methanogenic degradation pathway in rice field soil. Soil Biol. Biochem. 35, 1–8.
Frenzel, P., Bosse, U., Janssen, P.H., 1999. Rice roots and methanogenesis in a paddy soil: ferric iron as an alternative electron acceptor in the rooted soil. Soil Biol. Biochem. 31, 421–430.
Gilbert, B., Frenzel, P., 1998. Rice roots and CH_4 oxidation: the activity of bacteria, their distribution and the microenvironment. Soil Biol. Biochem. 30, 1903–1916.
Granberg, G., Ottosson-Lofvenius, M., Grip, H., Sundh, I., Nilsson, M., 2001. Effect of climatic variability from 1980 to 1997 on simulated methane emission from a boreal mixed mire in northern Sweden. Global Biogeochem. Cycles 15, 977–991.
Hosono, T., Nouchi, I., 1997. The dependence of methane transport in rice plants on the root zone temperature. Plant Soil 191, 233–240.
Huang, Y., Sass, R.L., Fisher, F.M., 1998a. Model estimates of methane emission from irrigated rice cultivation of China. Global Change Biol. 4, 809–821.
Huang, Y., Sass, R.L., Fisher, F.M., 1998b. A semi-empirical model of methane emission from flooded rice paddy soils. Global Change Biol. 4, 247–268.
IPCC, 1995. Climate change, 1994: radiative forcing of climate change and an evaluation of the IPCC IS92 emission scenarios. Cambridge University Press, Cambridge, England, New York, p. 339.
IPCC, 1995. IPCC Second Assessment Climate Change 1995.
Iversen, N., Jorgensen, B.B., 1985. Anaerobic methane oxidation rates at the sulfate methane transition in marine sediments from Kattegat and Skagerrak (Denmark). Limnol. Oceanogr. 30, 944–955.
Jaffe, P.R., Wang, S., Kallin, P.L., Smith, S.L., 2002. The dynamics of arsenic in saturated porous media: fate and transport modeling for deep aquatic sediments, wetland sediments, and groundwater environments. The Geochemical Society, Special Publication No. 7, pp. 379–398.
Jiao, Z.H., Hou, A.X., Shi, Y., Huang, G.H., Wang, Y.H., Chen, X., 2006. Water management influencing methane and nitrous oxide emissions from rice field in relation to soil redox and microbial community. Commun. Soil Sci. Plant Anal. 37, 1889–1903.
Jobbagy, E.G., Jackson, R.B., 2000. The vertical distribution of soil organic carbon and its relation to climate and vegetation. Ecol. Appl. 10, 423–436.
Kern, J.S., Gong, Z.T., Zhang, G.L., Zhuo, H.Z., Luo, G.B., 1997. Spatial analysis of methane emissions from paddy soils in China and the potential for emissions reduction. Nutr. Cycl. Agroecosyst. 49, 181–195.
Kettunen, A., 2003. Connecting methane fluxes to vegetation cover and water table fluctuations at microsite level: a modeling study. Global Biogeochem. Cycles 17, 1051.
Khalil, M.A.K., Rasmussen, R.A., Shearer, M.J., Dalluge, R.W., Ren, L.X., Duan, C.L., 1998a. Factors affecting methane emissions from rice fields. J. Geophys. Res. Atmos. 103, 25219–25231.
Khalil, M.A.K., Rasmussen, R.A., Shearer, M.J., Dalluge, R.W., Ren, L.X., Duan, C.L., 1998b. Measurements of methane emissions from rice fields in China. J. Geophys. Res. Atmos. 103, 25181–25210.
Kirk, G.J.D., 2003. Rice root properties for internal aeration and efficient nutrient acquisition in submerged soil. New Phytol. 159, 185–194.
Kirk, G.J.D., Du, L.V., 1997. Changes in rice root architecture, porosity, and oxygen and proton release under phosphorus deficiency. New Phytol. 135, 191–200.
Knox, J.W., Matthews, R.B., Wassmann, R., 2000. Using a crop/soil simulation model and GIS techniques to assess methane emissions from rice fields in Asia. III. Databases. Nutr. Cycl. Agroecosyst. 58, 179–199.
Kruger, M., Frenzel, P., Conrad, R., 2001. Microbial processes influencing methane emission from rice fields. Global Change Biol. 7, 49–63.
Li, C.S., Qiu, J.J., Frolking, S., Xiao, X.M., Salas, W., Moore, B., Boles, S., Huang, Y., Sass, R., 2002a. Reduced methane emissions from large-scale changes in water management of China's rice paddies during 1980–2000. Geophys. Res. Lett. 29, 1972.
Li, J., Wang, M.X., Huang, Y., Wang, Y.S., 2002b. New estimates of methane emissions from Chinese rice paddies. Nutr. Cycl. Agroecosyst. 64, 33–42.
Li, B.Z., Xin, W.J., Sun, S.B., Shen, Q.R., Xu, G.H., 2006. Physiological and molecular responses of nitrogen-starved rice plants to re-supply of different nitrogen sources. Plant Soil 287, 145–159.
Lu, Y., Wassmann, R., Neue, H.U., Huang, C., 1999. Impact of phosphorus supply on root exudation, aerenchyma formation and methane emission of rice plants. Biogeochemistry 47, 203–218.
Lu, Y.H., Wassmann, R., Neue, H.U., Huang, C.Y., 2000. Dynamics of dissolved organic carbon and methane emissions in a flooded rice soil. Soil Sci. Soc. Am. J. 64, 2011–2017.
Lu, Y.H., Watanabe, A., Kimura, M., 2002. Contribution of plant-derived carbon to soil microbial biomass dynamics in a paddy rice microcosm. Biol. Fertil. Soils 36, 136–142.
Matthews, R.B., Wassmann, R., Arah, J., 2000a. Using a crop/soil simulation model and GIS techniques to assess methane emissions from rice fields in Asia. I. Model development. Nutr. Cycl. Agroecosyst. 58, 141–159.
Matthews, R.B., Wassmann, R., Knox, J.W., Buendia, L.V., 2000b. Using a crop/soil simulation model and GIS techniques to assess methane emissions from rice fields in Asia. IV. Upscaling to national levels. Nutr. Cycl. Agroecosyst. 58, 201–217.
Megonigal, J.P., Schlesinger, W.H., 2002. Methane-limited methanotrophy in tidal freshwater swamps. Global Biogeochem. Cycles 16, 1088.
Minami, K., 1995. The effect of nitrogen-fertilizer use and other practices on methane emission from flooded rice. Fertilizer Res. 40, 71–84.
National Soil Survey of China, 1993–1996. Soil Species of China. China Agriculture Press, Beijing.
Nouchi, I., Mariko, S., Aoki, K., 1990. Mechanism of methane transport from the rhizosphere to the atmosphere through rice plants. Plant Physiol. 94, 59–66.
Nouchi, I., Hosono, T., Aoki, K., Minami, K., 1994. Seasonal-variation in methane flux from rice paddies associated with methane concentration in soil–water, rice biomass and temperature, and its modeling. Plant Soil 161, 195–208.

Park, S.S., Jaffe, P.R., 1996. Development of a sediment redox potential model for the assessment of post-depositional metal mobility. Ecol. Model. 91, 169–181.
Park, S.S., Jaffe, P.R., 1999. A numerical model to estimate sediment oxygen levels and demand. J. Environ. Qual. 28, 1219–1226.
Rodhe, H., 1990. A comparison of the contribution of various gases to the greenhouse-effect. Science 248, 1217–1219.
Roy, R., Kluber, H.D., Conrad, R., 1997. Early initiation of methane production in anoxic rice soil despite the presence of oxidants. FEMS Microbiol. Ecol. 24, 311–320.
Rubinigg, M., Stulen, I., Elzenga, J.T.M., Colmer, T.D., 2002. Spatial patterns of radial oxygen loss and nitrate net flux along adventitious roots of rice raised in aerated or stagnant solution. Funct. Plant Biol. 29, 1475–1481.
Schutz, H., Holzapfelpschorn, A., Conrad, R., Rennenberg, H., Seiler, W., 1989a. A 3-year continuous record on the influence of daytime, season, and fertilizer treatment on methane emission rates from an Italian rice paddy. J. Geophys. Res. Atmos. 94, 16405–16416.
Schutz, H., Seiler, W., Conrad, R., 1989b. Processes involved in formation and emission of methane in rice paddies. Biogeochemistry 7, 33–53.
Schutz, H., Seiler, W., Conrad, R., 1990. Influence of soil-temperature on methane emission from rice paddy fields. Biogeochemistry 11, 77–95.
Segers, R., 1998. Methane production and methane consumption: a review of processes underlying wetland methane fluxes. Biogeochemistry 41, 23–51.
Segers, R., Leffelaar, P.A., 2001a. Modeling methane fluxes in wetlands with gas-transporting plants. 1. Single-root scale. J. Geophys. Res. Atmos. 106, 3511–3528.
Segers, R., Leffelaar, P.A., 2001b. Modeling methane fluxes in wetlands with gas-transporting plants. 3. Plot scale. J. Geophys. Res. Atmos. 106, 3541–3558.
Segers, R., Rappoldt, C., Leffelaar, P.A., 2001. Modeling methane fluxes in wetlands with gas-transporting plants. 2. Soil layer scale. J. Geophys. Res. Atmos. 106, 3529–3540.
Singh, S., Kashyap, A.K., Singh, J.S., 1998. Methane flux in relation to growth and phenology of a high yielding rice variety as affected by fertilization. Plant Soil 201, 157–164.
Smith, S.L., Jaffe, P.R., 1998. Modeling the transport and reaction of trace metals in water-saturated soils and sediments. Water Resour. Res. 34, 3135–3147.
Strobel, B.W., 2001. Influence of vegetation on low-molecular-weight carboxylic acids in soil solution—a review. Geoderma 99, 169–198.
Stumm, W., Morgan, J.J., 1996. Aquatic Chemistry: Chemical Equilibria and Rates in Natural Waters. Wiley, New York, xvi, 1022 pp.
Ulgiati, S., Raugei, M., Bargigli, S., 2006. Overcoming the inadequacy of single-criterion approaches to life cycle assessment. Ecol. Model. 190, 432–442.
Van Bodegom, P.M., Scholten, J.C.M., 2001. Microbial processes of CH_4 production in a rice paddy soil: model and experimental validation. Geochim. Cosmochim. Acta 65, 2055–2066.
Van Bodegom, P.M., Stams, A.J.M., 1999. Effects of alternative electron acceptors and temperature on methanogenesis in rice paddy soils. Chemosphere 39, 167–182.
Van Bodegom, P., Goudriaan, J., Leffelaar, P., 2001a. A mechanistic model on methane oxidation in a rice rhizosphere. Biogeochemistry 55, 145–177.
Van Bodegom, P.M., Wassman, R., Metra-Corton, T.M., 2001b. A process-based model for methane emission predictions from flooded rice paddies. Global Biogeochem. Cycles 15, 247–263.
Van Bodegom, P.M., Verburg, P.H., van der Gon, A.C.D., 2002. Upscaling methane emissions from rice paddies: problems and possibilities. Global Biogeochem. Cycles 16, 1014.
Van Cappellen, P., Wang, Y.F., 1996. Cycling of iron and manganese in surface sediments: a general theory for the coupled transport and reaction of carbon, oxygen, nitrogen, sulfur, iron, and manganese. Am. J. Sci. 296, 197–243.
Walter, B.P., Heimann, M., 2000. A process-based, climate-sensitive model to derive methane emissions from natural wetlands: application to five wetland sites, sensitivity to model parameters, and climate. Global Biogeochem. Cycles 14, 745–765.
Wang, B., Adachi, K., 2000. Differences among rice cultivars in root exudation, methane oxidation, and populations of methanogenic and methanotrophic bacteria in relation to methane emission. Nutr. Cycl. Agroecosyst. 58, 349–356.
Wang, B., Neue, H.U., Samonte, H.P., 1997. Effect of cultivar difference ('IR72', 'IR65598' and 'Dular') on methane emission. Agric. Ecosyst. Environ. 62, 31–40.
Wang, B., Xu, Y., Wang, Z., Li, Z., Ding, Y., Guo, Y., 1999. Methane production potentials of twenty-eight rice soils in China. Biol. Fertil. Soils 29, 74–80.
Wang, S., Jaffe, P.R., Li, G., Wang, S.W., Rabitz, H.A., 2003. Simulating bioremediation of uranium-contaminated aquifers; uncertainty assessment of model parameters. J. Contam. Hydrol. 64, 283–307.
Wassmann, R., Neue, H.U., Lantin, R.S., Buendia, L.V., Rennenberg, H., 2000. Characterization of methane emissions from rice fields in Asia. I. Comparison among field sites in five countries. Nutr. Cycl. Agroecosyst. 58, 1–12.
Weiss, R., Shurpali, N.J., Sallantaus, T., Laiho, R., Laine, J., Alm, J., 2006. Simulation of water table level and peat temperatures in boreal peatlands. Ecol. Model. 192, 441–456.
Wissuwa, M., Ae, N., 2001. Further characterization of two QTLs that increase phosphorus uptake of rice (*Oryza sativa* L.) under phosphorus deficiency. Plant Soil 237, 275–286.
Wu, X.L., Chin, K.J., Stubner, S., Conrad, R., 2001. Functional patterns and temperature response of cellulose-fermenting microbial cultures containing different methanogenic communities. Appl. Microbiol. Biotechnol. 56, 212–219.
Wuebbles, D.J., Hayhoe, K., 2002. Atmospheric methane and global change. Earth Sci. Rev. 57, 177–210.
Wynn, T.M., Liehr, S.K., 2001. Development of a constructed subsurface-flow wetland simulation model. Ecol. Eng. 16, 519–536.
Xu, S.P., Jaffe, P.R., 2006. Effects of plants on the removal of hexavalent chromium in wetland sediments. J. Environ. Qual. 35, 334–341.
Xu, S., Leri, A.C., Myneni, S.C.B., Jaffe, P.R., 2004. Uptake of bromide by two wetland plants (*Typha latifolia* L. and *Phragmites australis* (Cav.) Trin. ex Steud). Environ. Sci. Technol. 38, 5642–5648.
Yan, X.Y., Ohara, T., Akimoto, H., 2003. Development of region-specific emission factors and estimation of methane emission from rice fields in the East, Southeast and South Asian countries. Global Change Biol. 9, 237–254.
Yan, X.Y., Yagi, K., Akiyama, H., Akimoto, H., 2005. Statistical analysis of the major variables controlling methane emission from rice fields. Global Change Biol. 11, 1131–1141.
Yang, S.S., Chang, H.L., 1999. Diurnal variation of methane emission from paddy fields at different growth stages of rice cultivation in Taiwan. Agric. Ecosyst. Environ. 76, 75–84.
Yao, H., Conrad, R., 2000. Effect of temperature on reduction of iron and production of carbon dioxide and methane in anoxic wetland rice soils. Biol. Fertil. Soils 32, 135–141.
Yu, K.W., Patrick, W.H., 2003. Redox range with minimum nitrous oxide and methane production in a rice soil under different pH. Soil Sci. Soc. Am. J. 67, 1952–1958.

Yu, Z.C., Campbell, I.D., Vitt, D.H., Apps, M.J., 2001. Modelling long-term peatland dynamics. I. Concepts, review, and proposed design. Ecol. Model. 145, 197–210.
Yue, T.X., Liu, J.Y., Jorgensen, S.E., Ye, Q.H., 2003. Landscape change detection of the newly created wetland in Yellow River Delta. Ecol. Model. 164, 21–31.
Zou, J.W., Huang, Y., Jiang, J.Y., Zheng, X.H., Sass, R.L., 2005. A 3-year field measurement of methane and nitrous oxide emissions from rice paddies in China: effects of water regime, crop residue, and fertilizer application. Global Biogeochem. Cycles 19, GB2021.